Paper ID: ICMIME2024_252

Impacts of Heat Transfer Coefficient and Pressure Drop of R32 with TiO_2 Nano-particle in a U-Bend Evaporator

Ahsan Habib[1], Dipayan Mondal[2,*], Md. Samir Hossen[2]
[1]Department of Chemical Engineering, Khulna University of Engineering & Technology, Khulna-9203, Bangladesh
[2]Department of Mechanical Engineering, Khulna University of Engineering & Technology, Khulna-9203, Bangladesh
E-mail: dipkuet@me.kuet.ac.bd

Abstract

The study explores the heat transfer coefficient and pressure drop of R32 refrigerant with the addition of TiO_2 nanoparticles flowing through a U-bend evaporator tube by a numerical study using ANSYS Fluent 2020. The U-bend geometry has a total length of 1000 mm, a bending radius of 10 mm, and a diameter of 8 mm. The mass flux of the TiO_2-R32 nano-fluid is varied across three values: 60 kg/m²s, 85 kg/m²s, and 160 kg/m²s. The influence of TiO_2 nanoparticle concentration on heat transfer is explored by considering concentrations of 1%, 2%, and 3%. The evaporator tube is modeled as copper, with a constant wall temperature of either 300 K or 350 K. At a mass flux of 160 kg/m²s, the heat transfer coefficient reaches its peak at 350 K for both R32 and TiO_2-R32. The maximum value is almost 60% higher at 350K than that observed at a temperature of 300 K. The pressure drop rises by 20% for R32 and 22.22% for TiO_2-R32 at 350 K. Flow regimes observed for both fluids include wavy annular flow, stratified flow, and bubbly flow. The scope of this work is to offer important insights into how the use of TiO_2 nano-fluid may improve the performance of refrigeration systems based on R32.

Keywords: TiO_2-R32 nano-fluid; U-bend tube evaporator; Heat transfer coefficient; Flow pattern, Frictional pressure drop

1. Introduction

Evaporators act as heat transfer agents, taking heat from colder spaces and passing it to a refrigerant with a higher temperature. Traditionally, HFC134a has been a popular refrigerant choice, but concerns about its environmental impact have driven the search for alternatives. R-32, a cutting-edge refrigerant, has a low environmental impact, both in terms of global warming and ozone depletion, positioning it as a favorable option [1], [2]. By the way, the work explores the potential of enhancing R32 performance through the use of nanotechnology. Specifically, we investigate the heat transfer characteristics of R32 mixed with titanium oxide (TiO_2) nanoparticles flowing through a U-bend evaporator tube using numerical analysis. U-bend tubes, while promoting compactness in heat exchanger design, introduce complexities in flow patterns and heat transfer [3]–[6].

Numerous researchers have studied pressure drop, heat transfer, and flow patterns in adiabatic and diabatic conditions in U-bend tubes with various orientations. Still, there is a lack of research on U-bend tubes, especially when it comes to diabatic conditions, and few studies have been done on mapping the flow pattern in U-bend tubes. Oh and Son [7] investigated heat transmission for R134a and R22 refrigerants in flat copper conduits (diameters: 1.77-5.35 mm). They found that smaller diameters affected the heat transfer coefficient (varying heat fluxes, vapor qualities, mass flow rates, and saturation temperatures). Shiferaw et al. [8] studied flow in tubes with different diameters (2.01 mm and 4.26 mm) using R134a refrigerant. They found that the larger diameter tube resulted in higher vapor quality (40-50% vs. 20-30%). Islam et al [9] conducted a computer-aided design (CFD) study integrating the flow boiling evaporation and flow patterns of R32 and R1234yf with Al_2O_3 nanoparticles in a U-bend tube evaporator. The study focused on mass fluxes ranging from 35 kg/m²s to 160 kg/m²s at a saturation temperature of 273.15 K, and a curvature ratio for downward-oriented flow. Huang and Wang [10] explored single-phase flow in parallel flow heat exchangers with rectangular inlet and exit headers. They found that the last tube's flow rate was just half that of the first few and that utilizing smaller tubes, or a wider entry distance might improve the improper distribution.

This research seeks to investigate how the effectiveness of a U-bend evaporator using R32 with TiO_2 nanoparticles is affected by various factors like flow rate, nanoparticle concentration, and tube temperature. The findings will contribute valuable insights into optimizing R32-based refrigeration systems for improved efficiency and environmental sustainability.

2. Methodology

The mathematical model of refrigerant flow boiling simulates the behavior of a two-phase system. The model assumes a steady, three-dimensional flow of an incompressible fluid with a constant temperature along the copper evaporator tube.

2.1 Governing equation

The continuity formula is:

$$\frac{\partial}{\partial t}(\alpha_q \rho_q) + \nabla \cdot (\alpha_q \rho_q \vec{v}_q) = \sum_{p=1}^{n} (\dot{m}_{pq}) \quad (1)$$

The method of weighted summation of volume fractions is employed to ascertain the physical properties of fluids, including viscosity and density, which can be illustrated by Eqs. (2) and (3).

$$\rho = \alpha_l \rho_l + \alpha_v \rho_v \quad (2)$$

$$\mu = \alpha_l \mu_l + \alpha_v \mu_v \quad (3)$$

where the symbols α_v, α_l, ρ_v, ρ_l, μ_v, and μ_l represent the volume fractions, densities, and viscosities of the vapor and liquid phases, respectively. The momentum equation is solved by the VOF model, where $\vec{v}$ is the velocity vector caused by the phase change process [11]. The following momentum equation is expressed as Eq. (4).

$$\frac{\partial}{\partial t}(\rho \vec{v}) + \nabla(\rho \vec{v} \vec{v}) = -\nabla p + \rho \vec{g} + \nabla \left[\mu (\nabla \vec{v} + \nabla v^T) - \frac{2}{3}\mu \nabla \vec{v} I\right] + F_{CSF} \quad (4)$$

where $\vec{g}$ represents the acceleration due to gravity, while P, I, and F_{CSF} express the pressure, unit tensor, and surface tension, respectively. The model of continuum surface force (CSF) is utilized to estimate the surface force for the vapor and liquid phase, which is written in Eq. (5).

$$F_{CSF} = 2\sigma \frac{\alpha_l \rho_l C_v \nabla \alpha_v + \alpha_v \rho_v C_l \nabla \alpha_l}{\rho_l + \rho_v} \quad (5)$$

where σ represents the coefficient of surface tension, while C_l and C_v present the surface curvature for liquid and vapor, respectively. All phase components within the control volume have the same energy equation, which can be written as follows:

$$\frac{\partial}{\partial t}(\rho E) + \nabla[(\rho E + P)\vec{v}] = \nabla.(\lambda \nabla T) + S_e \quad (6)$$

In the equation, λ represents the average heat transfer ability of the two phases, T is their average temperature, and S_e is the energy change caused by the phase change. Again,

$$E = \frac{\alpha_l \rho_l E_l + \alpha_v \rho_v E_v}{\alpha_l \rho_l + \alpha_v \rho_v} \quad (7)$$

The evaporation-condensation model is a physics-based mechanistic model that is accessible through both the mixture and Eulerian multiphase models. It describes mass transfer based on specific temperature regimes, as follows:

$$if\ T > T_{sat}, \quad m_{e \to v} = coeff * \alpha_1 p_1 \frac{(T - T_{sat})}{T_{sat}} \quad (8)$$

$$if\ T < T_{sat}, \quad m_{e \to v} = coeff * \alpha_v p_v \frac{(T - T_{sat})}{T_{sat}} \quad (9)$$

2.2 Geometry and meshing

Fig. 1 shows the geometry of a 3D model U-bend tube evaporator, while Fig. 2 shows the meshing of the considered geometry. However, the geometry dimension length, bend radius, diameter are respectively 1000mm, 10 mm, 8mm. Tetrahedral mesh is applied to the fluid domain. The elements and nodes are respectively 456104, 143529 with the orthogonal quality measurement 0.71819.

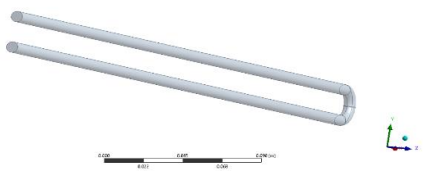


Fig. 1. 3D model of U bend tube.

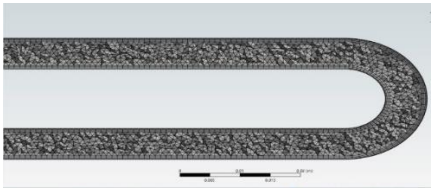


Fig. 2. Tetrahedral meshing.

2.3 Boundary conditions and validation

The properties of R32 were obtained from a reliable database called REFPROP 10.0, as shown in Table 1. While, the boundary conditions used in this study are specified in Table 2. The model was validated with Oudah et al.

[12] where the tube was 1m long made from copper, as shown in Fig. 3. To validate the findings, the correlation between vapor quality and coefficient of heat transfer was compared to the work of Oudah et al. [12] work.

Table 1. Features of R32, Tsat= 270.15K, P= 0.7377 MPa respectively [13], [14].

Properties	R32	
	Liquid	**Vapor**
Density (kg/m^3)	1065.5	20.044
Specific heat capacity (J/kg K)	1729.7	1220.8
Thermal conductivity $\times 10^{-2}$ (W/ m.K)	14.7	1.14
Viscosity $\times 10^{-5}$ (kg/m.s)	15.561	1.137
Surface tension $\times 10^{-2}$ (N/m)	1.1507	1.1507
Molecular weight (kg/kmol)	52	52

Table 2. Boundary conditions

Items	**Value and/or type**
Wall boundary	Constant temperature
Type	Wall
Phase	Solid
Temperature (K)	350.15
Inlet Boundary	
Type	Velocity inlet
Phase	R-134a liquid
Inlet Temperature (K)	267.65
Velocity (m/s)	0.1
Phase	R-134a liquid
Vapor fraction	0
Outlet- boundary	
Type	Pressure outlet
Operating Pressure (Pa)	262360

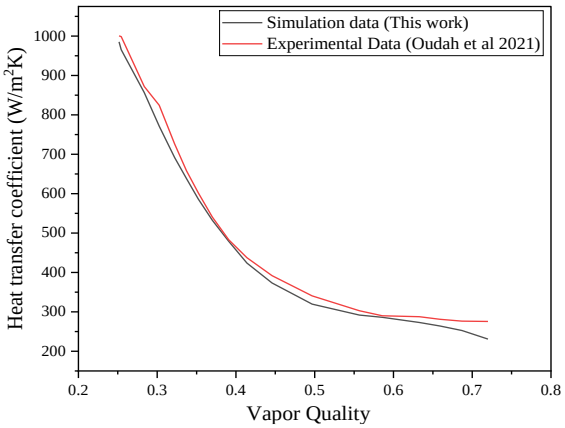


Fig. 3. Validation of this simulated work with Experimental data (Oudah et al. [12])

3. Results and discussion

3.1 Mass fluxes effect on R32

Fig. 4(a) and Fig. 4(b illustrate the variation of heat transfer coefficient in relation to R32 vapor quality for different mass fluxes at 300K and 350K, respectively.

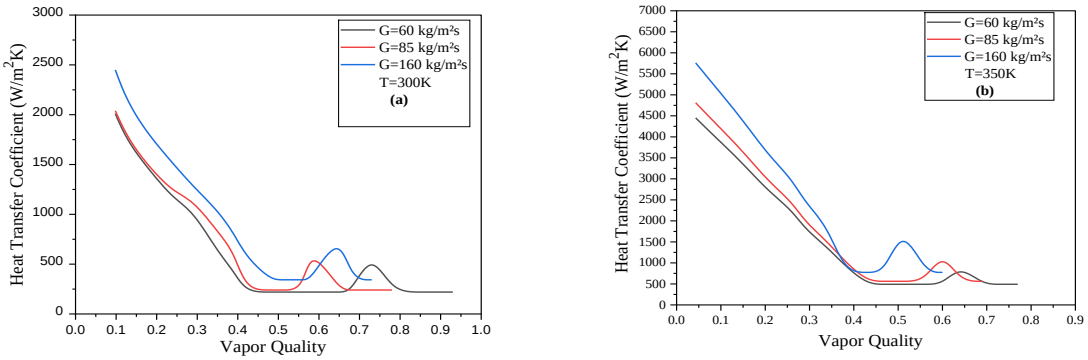


Fig. 4. Heat transfer coefficient in relation to R32 vapor quality for different mass fluxes: (a) at 300K and (b) at 350K.

During boiling evaporation, the mass flux and vapor percentage have a significant impact on the average heat transfer coefficient of R32 when it flows through a U-bend tube with a downward flow. The average heat transfer coefficient value is affected by changing the mass flow value, which are 60, 85, and 160 kg/m^{2}s at a given temperature. When mass flux is exactly 160 kg/m^{2}s, the coefficient of heat transfer is at its maximum for all temperature scenarios because of the significant contribution of convective evaporation under force. The maximum value is almost 60% higher at 350K than that observed at a temperature of 300 K. The transmission of heat changes slightly along the tube. The transition from stratified to annular flow and the flow's separation both contribute to the increase in heat transmission. Following the bend, heat transmission continues to decline as the flow becomes stratified once more.

3.2 Frictional pressure drop of R32

The resistive pressure drop rises with mass fluxes in accordance with the vapor's quality, as seen in Figs. 5(a) and 5(b). Because of decreasing density of R32 for two phases, the vapor displacement exceeds the liquid film velocity. Higher resistive pressure losses and increased shear stress are the outcomes of this phenomena. As mass flow rises, so does the resistive pressure increases. This is caused by increasing contact shear stress within the R32 both liquid and vapor phases and the tube wall in the two-phase fluid. Compared to the lesser mass fluxes, a mass flow of 160 kg/m2s was shown to result in a greater drop in frictional pressure.

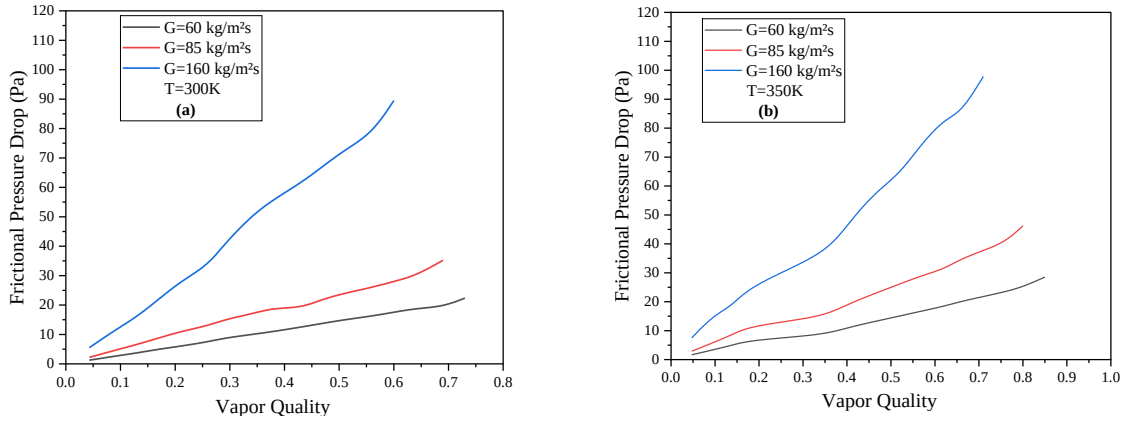


Fig. 5. Frictional pressure drops for different mass fluxes of R32 with the vapor quality: (a) at 300K and (b) at 350K.

3.3 Mass flux effect on TiO_2-R32 nanofluid

The mass flux and vapor percentage during the flow boiling evaporation of TiO_2-R32 nanofluid in a curved tube with downhill flow have a major effect on the coefficient of heat transfer. The effects of varying the nanoparticle percentage in a mixture of R32 refrigerant and TiO_2 nanoparticles (from 1 vf% to 3 vf%) at a constant temperature on the coefficient of heat transfers are shown in Figs. 6(a) and 6(b).

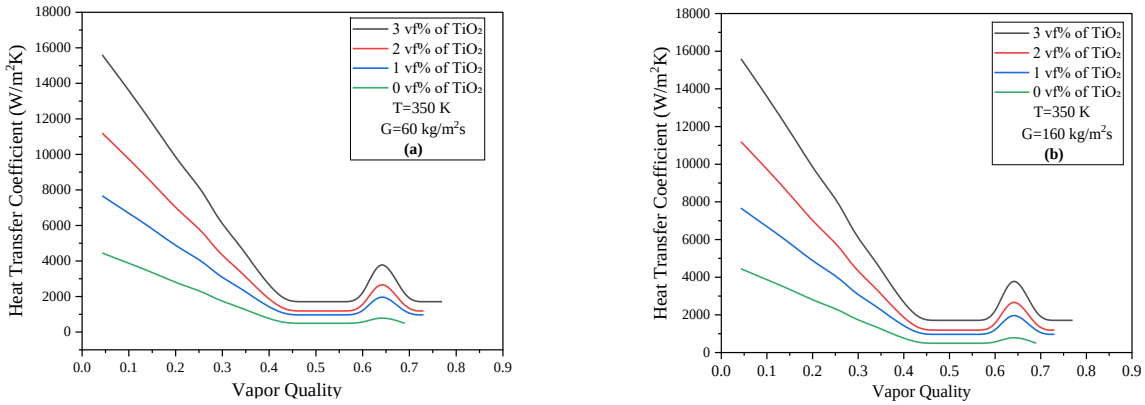


Fig. 6. Heat transfer coefficient for different percentage of TiO_2-R32 nanofluid at constant mass flux: (a) 60 kg/m^{2}s and (b) 160 kg/m^{2}s.

Due to their enhanced thermal conductivity, in this constant temperature situations, the coefficient of heat transfer is reached maximum at 3% concentration of TiO_2 nanoparticles. The observation is evident that the combination of nanofluid and refrigerant at varying proportions notably enhanced the average coefficient of heat transfer to a significant extent, as well as the vapor fraction. There are specific alterations in the coefficient of heat transfer at the curve. The separation of the flow and the transition from stratified to annular flow, which encourages convective heat transfer, are the causes of this phenomenon. After the curve, when the flow resumes its stratified flow, there is an additional reduction in heat transmission.

3.4 Frictional pressure drop of TiO_2-R32

As the vapor quality rises, so does the resistive pressure drop increase, as Figs. 7(a) and 7(b) demonstrate the frictional pressure drop with varying the TiO_2 at 300K and 350K. At a mass flux of 160 kg/m²s, the pressure drop rises by 20% for R32 and 22.22% for TiO_2-R32 wherein the 3% TiO_2 is considered at 350 K compared to 300 K. This is because the velocity of vapor surpasses the liquid film velocity when the density of the two phases of TiO_2-R32 nanofluid falls. Higher resistive pressure losses and increased shear stress are the outcomes of this. Resistive pressure loss also rises as mass flow increases. The increased friction between the nanofluid and the tube wall, as well as between the liquid and gas parts of the nanofluid, is causing this problem.

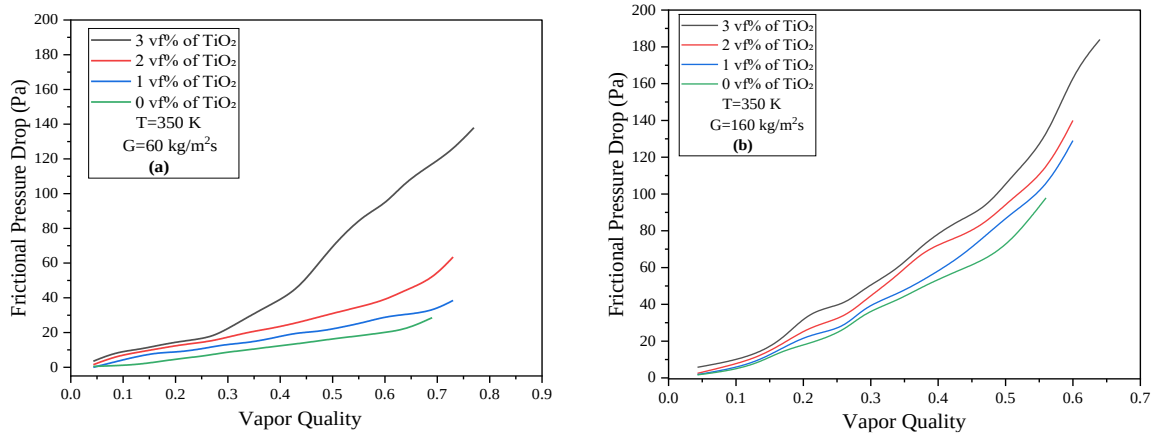


Fig. 7. Frictional pressure drop of TiO_2-R32 nanofluid at constant mass flux: (a) 60 kg/m²s and (b) 160 kg/m²s.

3.5 Flow pattern

The illustration showcases from Fig. 8 to Fig. 9 the boiling process of the R32 and TiO_2-R32 mixture within a U-bend tube. It highlights the influence of temperature (350 K) on initiating evaporation near the tube wall. The observed flow patterns include stratified (layered) and annular flow, significantly impacted by gravity. The vapor fraction ranges from 0.1 to 0.83, with distinct flow regimes across this range. The U-bend section exhibits complex flow due to vapor-liquid overlap. Notably, the nanofluid mixture demonstrates faster phase change and enhanced heat transfer compared to the pure refrigerant. In summary, R32 and TiO2-R32 exhibit peak heat transfer coefficients at 350 K and flow regimes encompassing wavy annular, stratified, and bubbly flow.

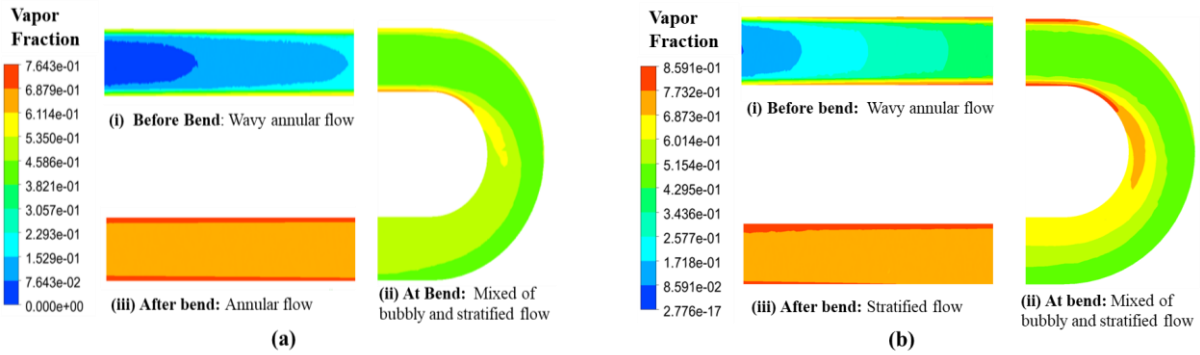


Fig. 8. Illustration for flow pattern when the mass flux of G=160 kg/m²s at T=350 K: (a) R32, and (b) TiO_2-R32.

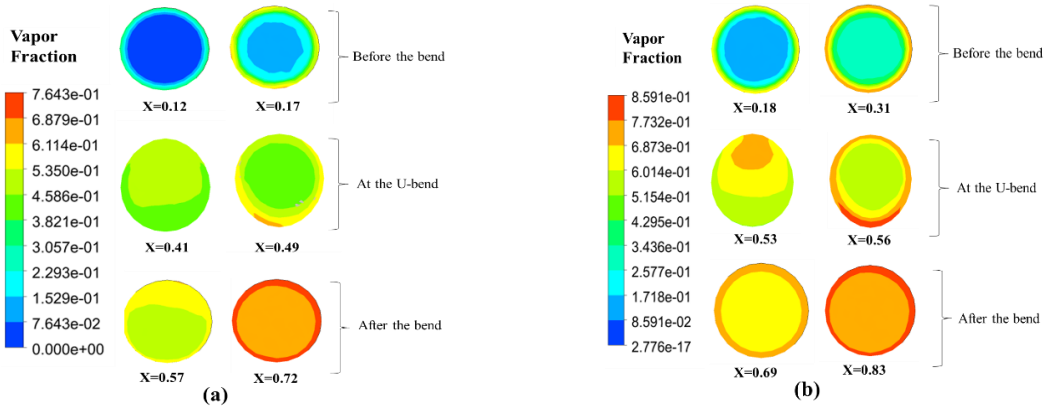


Fig. 9. Flow form and vapor quality occurred before, at bend, and after bend for: (a) R32 and (b) TiO_2-R32.

4. Conclusion

This numerical analysis, conducted using ANSYS Fluent 2020, investigated the characteristics of heat transfer of R32 refrigerant with TiO_2 nanoparticles (concentrations of 1%, 2%, and 3%) flowing through a U-bend evaporator tube. The study explored the influence of mass flux (60, 85, and 160 kg/m²s), evaporator wall temperature (300 K and 350 K), and nanoparticle concentration on heat transfer. The specific findings are as follows:

- At a mass flux of 160 kg/m²s, the heat transfer coefficient reaches its maximum value across all temperature ranges due to the significant contribution of forced convective evaporation. R32 and TiO2-R32 exhibit peak heat transfer coefficients at 350 K and achieved 60% higher than observed at 300 K.
- The pressure drop rises by 20% for R32 and 22.22% for TiO_2-R32 (considering 3% TiO_2) at 350 K rather than 300 K when comparing mass fluxes of 160 kg/m²s and 60 kg/m²s.
- The flow through the U-bend tube was observed to consist of three distinct flow regimes encompassing wavy annular, stratified, and bubbly flow.

5. Acknowledgement

The Khulna University of Engineering & Technology is acknowledged with heartfelt thanks by the authors for supplying high-performance computing resources.

6. References

[1] J. Zhang, W. Li, and W. J. Minkowycz, "Numerical simulation of condensation for R410A at a different saturation temperature in mini/micro tubes," *Numer. Heat Transf. Part A Appl.*, vol. 69, no. 8, pp. 825–840, 2016.

[2] R. Chandrasekar, T. Raja, J. Santhosh, and S. Arunkumar, "Numerical Analysis of Heat Transfer in Refrigerant Flow Through a Condenser Tube," *Int. J. Res. Eng. Technol.*, vol. 03, no. 11, pp. 37–42, 2014.

[3] Z. Cao, H. Zhang, H. Mei, G. Yan, W. Chu, and Q. Wang, "Numerical Study on R32 Flow Condensation in Horizontally Oriented Tubes with U-Bends," *Energies*, vol. 15, no. 13, 2022.

[4] K. Pasha, "Controlling the Nusselt Number in a TiO2/R134a Nano-refrigerant System," *Int. J. Heat Technol.*, vol. 37, no. 1, pp. 179–187, 2019.

[5] O. A. Alawi, N. A. C. Sidik, and A. S. Kherbeet, "The effects of nanolubricants on boiling and two phase flow phenomena: A review," *Int. Commun. Heat Mass Transf.*, vol. 75, pp. 197–205, 2016.

[6] V. Trisaksri and S. Wongwises, "Nucleate pool boiling heat transfer of TiO2–R141b nanofluids," *Int. J. Heat Mass Transf.*, vol. 52, no. 5–6, pp. 1582–1588, 2009.

[7] K.-I. Choi, A. S. Pamitran, C.-Y. Oh, and J.-T. Oh, "Boiling heat transfer of R-22, R-134a, and CO_2 in horizontal smooth minichannels," *Int. J. Refrig.*, vol. 30, no. 8, pp. 1336–1346, 2007.

[8] D. Shiferaw, T. G. Karayiannis, and D. B. R. Kenning, "Flow boiling in a 1.1 mm tube with R134a: Experimental results and comparison with model," *Int. J. Therm. Sci.*, vol. 48, no. 2, pp. 331–341, 2009.

[9] L. Islam, D. Mondal, A. Islam, and P. Das, "Effects of Heat Transfer Characteristics of R32 and R1234yf with Al_2O_3 Nanoparticle through U-Bend Tube Evaporator," *J. Eng.*, vol. 2024, pp. 24, Art ID 9991809, 2024.

[10] C. H. Huang and C. H. Wang, "The design of uniform tube flow rates for Z-type compact parallel flow heat exchangers," *Int. J. Heat Mass Transf.*, vol. 57, no. 2, pp. 608–622, 2013.

[11] C. W. Hirt and B. D. Nichols, "Volume of Fluid (VOF) Method for the Dynamics of Free Boundaries*," *J. Comput. Phys. 39*, vol. 201–225, 1981.

[12] M. H. Oudah, M. K. Mejbel, and M. K. Allawi, "R134a flow boiling heat transfer (FBHT) characteristics in a refrigeration system," *J. Mech. Eng. Res. Dev, vol. 44, no. 4, pp. 69-83*, 2021.

[13] "E. W. Lemmon, I. H. Bell, M. L. Huber, and M. O. McLinden, NIST Standard Reference Database 23: Reference Fluid Thermodynamic Properties-REFPROP (DLL Version 10.0a) ", NIST, USA, 2018.

[14] M. L. Huber, "Models for viscosity, thermal conductivity, and surface tension of selected pure fluids as implemented in REFPROP v10.0", p. NISTIR8209, 2018.